

**THE RIGOROUS CAD OF APERTURE-COUPLED T-JUNCTION
BANDSTOP-FILTERS, E-PLANE CIRCUIT ELLIPTIC-FUNCTION FILTERS,
AND DIPLEXERS**

F. Arndt, and T. Sieverding

Microwave Department, University of Bremen
Kufsteiner Str., NW1, D-2800 Bremen, W.-Germany

ABSTRACT

The rigorous CAD of waveguide bandstop-filters, of elliptic-function E-plane integrated circuit filters with additional bandstop cavities, and of high return loss E-plane T-junction diplexers with iris matching elements is introduced. Based on the general rectangular waveguide T-junction key-building block modal S-matrix, the design takes into account both the finite thickness of all coupling elements and the higher order mode interaction at all step discontinuities. The theory is verified by measurements.

INTRODUCTION

The aperture-coupled T-junction is a useful circuit element [1] - [6] often utilized in rectangular waveguide components for many applications, such as for the design of bandstop-filters [2], manifold multiplexers [4], or couplers [5]. Many refined theories are available [1], [2], [4] - [6] for deriving the equivalent circuit for such structures. However, the increasing demand for compact and low-cost components as well as the growing interest in the millimeter wave frequencies have prompted the need for more accurate methods which take adequately into account the finite thicknesses and the higher-order mode interactions of all discontinuities involved, and which allow to avoid additional tuning screws. Although an exact calculation for the rectangular waveguide T-junction equivalent circuit parameters is available for a long time [3], no rigorous analysis for the general aperture-coupled T-junction, as well as for the components utilizing this circuit element, has been derived so far.

The purpose of this paper is to present a suitable computer-aided design method for the class of waveguide components shown in Fig. 1, where the cavities or filter sections, respectively, are combined by aperture-coupled T-junctions: The bandstop resonator cavity filter (Fig. 1b), the E-plane integrated

circuit filter with additional aperture-coupled bandstop cavities (Fig. 1c), and the E-plane T-junction diplexer with iris matching elements (Fig. 1d). The design method is based on field expansion into the complete set of eigenmodes which yield directly the modal S-matrix of the T-junction key-building block discontinuity (Fig. 1a). The combination with the already known modal S-matrices, e.g. the double-step discontinuity [7] and the septated waveguide section [8], achieves the rigorous description of the composed circuits, such as the aperture-coupled T-junction element, and the complete filter or diplexer structure.

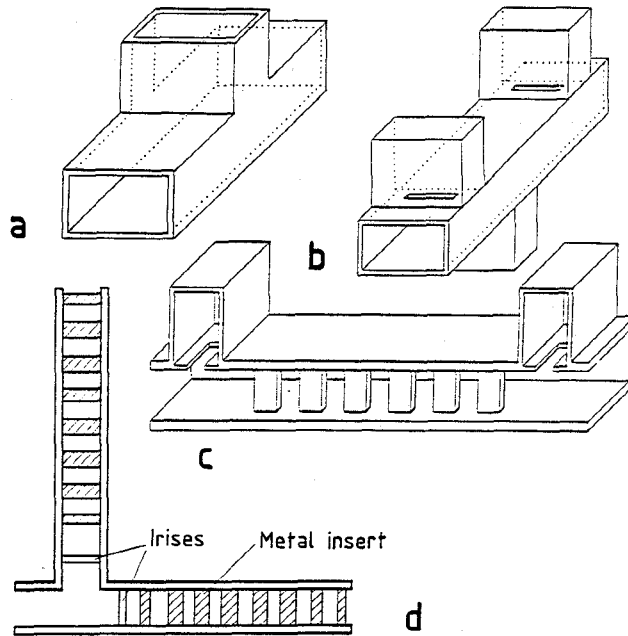


Fig. 1: The class of waveguide components investigated

- a) T-junction key-building block element.
- b) Bandstop resonator cavity filter.
- c) E-plane integrated circuit filter with aperture-coupled bandstop cavities.
- d) The E-plane T-junction diplexer with iris matching elements.

The method includes the higher-order mode coupling effects, the finite thickness of all obstacles, and allows the passband and stopband characteristics of the filters or diplexers under investigation to be considered in the design. For computer optimization, the evolution strategy method [8], [10] is applied. Computer-optimized design examples are presented which demonstrate the efficiency of the described design method: 1) a three-resonator bandstop filter in the waveguide X-band (8 - 12 GHz) with high peak stopband attenuation, 2) an E-plane metal insert filter with aperture-coupled stopband resonator sections which achieves an elliptic function behavior together with high return loss and - in contrast to metal insert coupled resonators [9] - high attenuation values over a broad frequency band, and 3) an inductively matched E-band (60 - 90 GHz) E-plane T-junction metal insert diplexer with high return loss and stopband attenuation. The theory is verified by measurements.

THEORY

For the rigorous computer-aided design of the structures to be investigated (Fig. 1), the modal S-matrix method [7] - [10] is applied, where the involved sections are decomposed into appropriate key building blocks including the general T-junction (Fig. 2). The combination with the already known modal S-matrices, e.g. the double-step discontinuity [7] and the metal insert section [8], achieves the rigorous description of the composed circuits, such as the aperture-coupled T-junction element and the complete filter or diplexer component, respectively. The inclusion of the also known scattering matrices of a homogeneous waveguide section allows one to consider adequately the finite iris thickness. The total scattering matrix of the components (Fig. 1) is formulated by suitable direct combination of the individual modal S-matrices by an iteration process described in [8] which requires only one matrix inversion, preserves numerical accuracy, and requires no symmetry of modes.

Since the known rigorous calculations of the T-junction element have been restricted hitherto to the cases of pure E-plane [10] and H-plane junctions [8], or on the equivalent-circuit admittance matrix [3], the investigation of the structures of Fig. 1 requires the derivation of the general six-field component modal S-matrix of the T-junction key-building block discontinuity (Fig. 2). The fields

$$\mathbf{E} = \frac{1}{j\omega\epsilon} \nabla \times \nabla \times (\mathbf{Q}_{ez}) + \nabla \times (\mathbf{Q}_{hz}) \quad (1)$$

$$\mathbf{H} = -\frac{1}{j\omega\mu} \nabla \times \nabla \times (\mathbf{Q}_{hz}) + \nabla \times (\mathbf{Q}_{ez})$$

in the homogeneous subregions I, II, III (Fig. 2) are derived from the z-components of the electric (e) and magnetic (h) vector potentials, respectively,

$$\mathbf{Q}_{ez,y}^o = \sum_{i^o} N_{i^o}^o \cdot T_{ei^o}^o \cdot (A_{ei^o}^o, B_{ei^o}^o) \cdot e^{jk_{ze}^o z, y} \quad (2)$$

$$\mathbf{Q}_{hz,y}^o = \sum_{i^o} N_{i^o}^o \cdot T_{hi^o}^o \cdot (A_{hi^o}^o, B_{hi^o}^o) \cdot e^{jk_{zh}^o z, y}$$

where $o = I, II, III$ (number of subregions), i^o is the index for all TE- and TM-modes in each subregion, N are the normalization factors due to the complex power, and T are the eigenfunctions in the corresponding subregions, analogous to [7] - [10]. A are the amplitude coefficients of the forward (-), B of the backward (+) waves, and k_{zh}^o , k_{ze}^o are the wavenumbers of the corresponding TE- and TM-modes, respectively. The field in the cavity subregion IV (Fig. 2) is superimposed by three suitably chosen standing wave solutions [10], where solution 1 is obtained if the boundary planes P_2 and P_3 are short-circuited and P_1 is open; solutions 2 and 3 are found analogously.

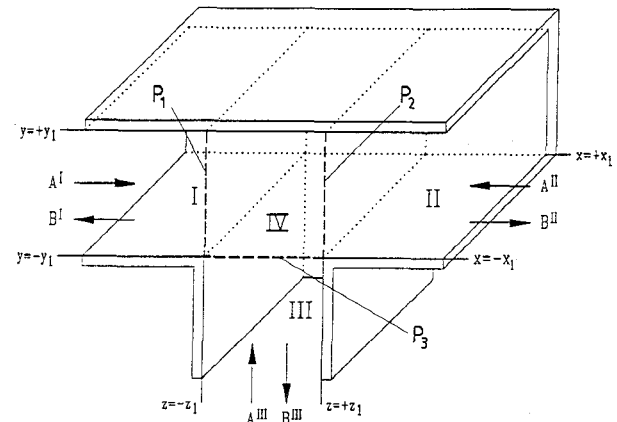


Fig. 2:
General six-field component T-junction key-building block discontinuity.

By matching the tangential field components given by (1), (2) at the common interfaces across the discontinuities, and utilizing the orthogonal property of the modes the still unknown amplitude coefficients can be related to each other in the form of the desired modal S-matrix (S^T) of the T-junction

$$(B) = (S^T) (A) . \quad (3)$$

A computer program was written using the preceding relations and utilizing the evolution strategy method, cf. [8], [10], for optimizing the geometrical parameters for given specifications. For the optimization, sufficient asymptotic behavior has been obtained by consideration of 18 TE- and TM-modes for the general key-building block junctions. The final design results are verified by an inclusion of 45 TM- and TE-modes.

RESULTS

For the example of a WR-137 (34.85mm \times 15.799mm) rectangular waveguide T-junction with a reduced width (WR-90: 22.86mm \times 10.16mm) side waveguide (port 3), Figs. 3 show the comparison between the scattering parameters obtained by our modal-S-matrix method and by the exact equivalent circuit admittance matrix calculation by Sharp [3] which has been verified there also by measurements. Good agreement may be stated. The power coupling mechanism below and above the cutoff frequency of the side waveguide may be clearly identified.

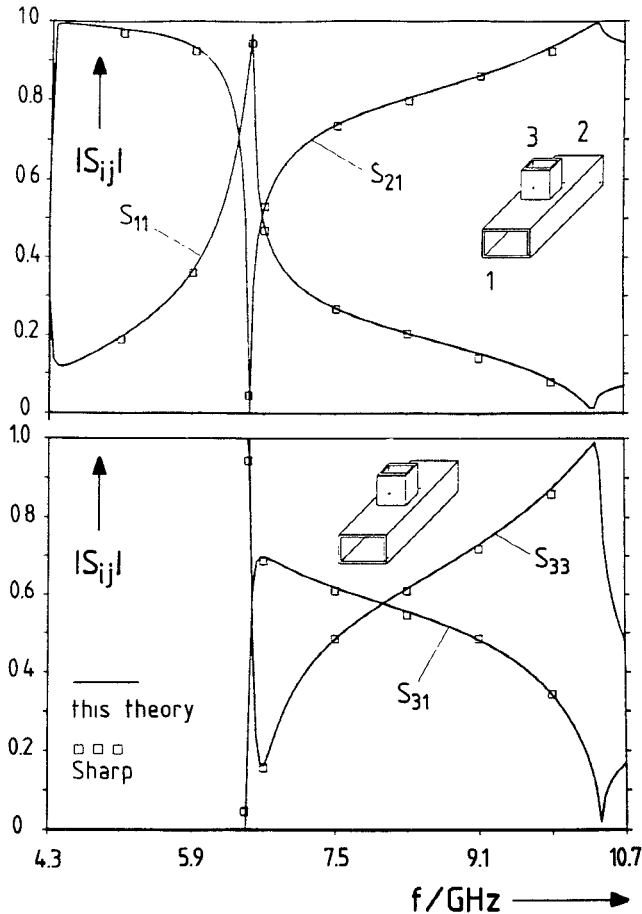


Fig. 3:
WR-137 (34.85mm \times 15.799mm) T-junction
with a reduced width (WR-90: 22.86mm \times
10.16mm) side waveguide (port 3).

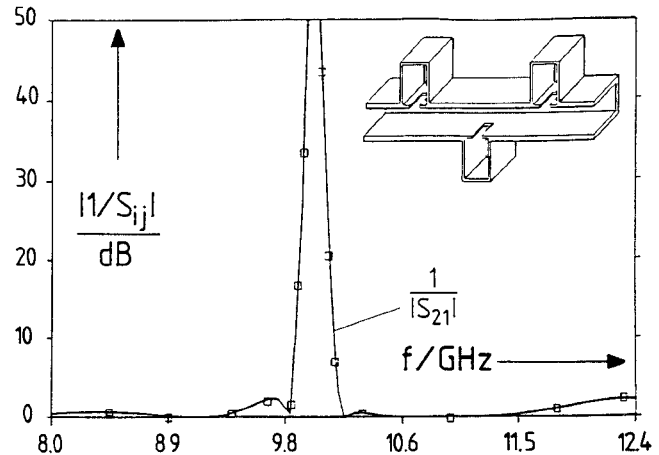


Fig. 4:
Insertion loss of an X-band (WR-90:
22.86mm \times 10.16mm) bandstop filter

A waveguide bandstop filter is conveniently realized [2] using aperture-coupled resonators connected in series and spaced an odd multiple of a quarter wavelength apart. Three-quarter intervals, instead of one-quarter spacing, is preferred [2] in order to reduce the otherwise strong interaction which would cause three peaks of high attenuation, instead of the desired single narrow-band peak. In order to verify the design theory presented in this paper also by a more complicated structure, Fig. 4 shows the calculated and measured insertion and return loss, respectively, of an X-band (WR-90 waveguide) bandstop filter example which has been constructed by using nearly the same dimensions as given in [2], but without the tuning screws. Very good agreement between our calculations and measurements may be stated.

For many purposes, such as for channel filters, when frequency selectivity and high stopband attenuation over a broad frequency band are considered to be important filter properties, it may be highly desirable to improve the rejection quality of standard direct coupled cavity bandpass filters. Fig. 5 presents the computer-optimized design results of a Ku-band (WR-62 waveguide: 15.799mm \times 7.899mm) metal-insert filter with additional aperture-coupled bandstop cavities. The filter shows elliptic-function behavior similar to the dual-mode approach of orthogonal mode filters [11], and avoids the disadvantage of the relatively small second stopband of the metal-insert coupled type [9]; this is due to the reduced interactions of the aperture-coupled cavities with the main filter section, in comparison with [9]. Moreover, very good return loss behavior is achieved by this design.

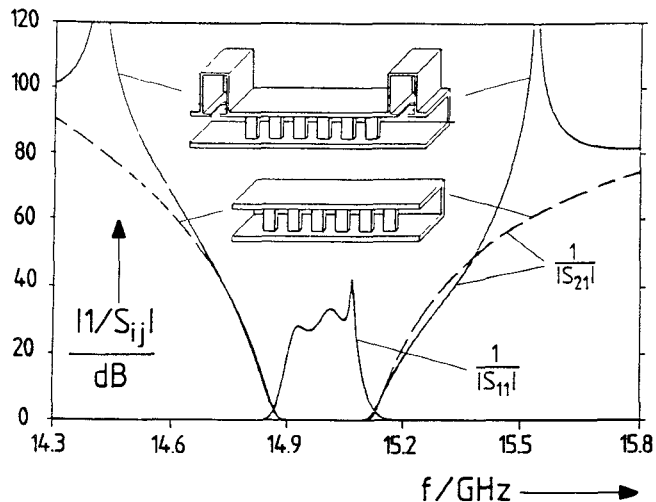


Fig. 5:
Computer-optimized design results of a Ku-band (WR-62: 15.799mm \times 7.899mm) elliptic-function-type metal-insert filter.

Figs. 6 show the computer-optimized design results of E-plane T-junction coupled metal insert diplexers. Very good agreement between the theoretically predicted values and the measurements may be stated for the realized X-band type (Fig. 6a). Additional matching irises with optimized dimensions and distance to the first filter sections achieve diplexers with excellent return loss behavior. This is demonstrated with the E-band (WR-12 waveguide: 3.099mm \times 1.549mm) diplexer example presented in Fig. 6b which achieves overall 26dB return loss within both passbands.

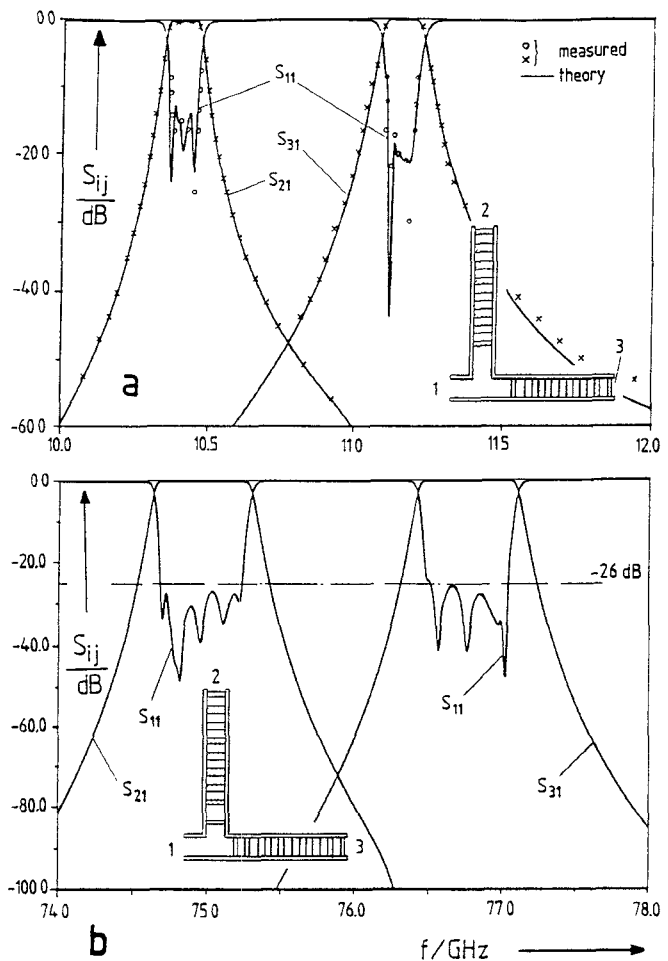


Fig. 6:
Computer-optimized design results of E-plane T-junction coupled metal insert diplexers.

- a) X-band (WR-90: 22.86mm \times 10.16mm).
- b) E-band (WR-12: 3.099mm \times 1.549mm) diplexer with additional matching irises

REFERENCES

- [1] N. Marcuvitz, "Waveguide Handbook". New York: McGraw-Hill, 1951.
- [2] L. Matthaei, L. Young, and E.M.T. Jones, "Microwave Filters, Impedance Matching Networks, and Coupling Structures". New York: McGraw-Hill, 1964.
- [3] E.D. Sharp, "An exact calculation for a T-junction of rectangular waveguides having arbitrary cross sections". IEEE Trans. Microwave Theory Tech., vol. MTT-15, pp. 109 - 116, Feb. 1967.
- [4] J.D. Rhodes, and R. Levy, "Design of general manifold multiplexers", IEEE Trans. Microwave Theory Tech., vol. MTT-27, pp. 111 - 123, Feb. 1979.
- [5] R. Levy, "Improved single and multiaperture waveguide coupling theory, including explanation of mutual interactions", IEEE Trans. Microwave Theory Tech., vol. MTT-28, pp. 331 - 338, April 1980.
- [6] B.N. Das, N.V.S. Narashima Sarma, and A. Chakraborty, "A rigorous variational formulation of an H plane slot-coupled Tee junction", IEEE Trans. IEEE Trans. Microwave Theory Tech., vol. MTT-38, pp. 93 - 95, Jan. 1990.
- [7] H. Patzelt, and F. Arndt, "Double-plane steps in rectangular waveguides and their application for transformers, irises, and filters", IEEE Trans. IEEE Trans. Microwave Theory Tech., vol. MTT-30, pp. 771-776, May 1982.
- [8] J. Dittloff, and F. Arndt, "Rigorous field theory design of millimeter-wave E-plane integrated circuit multiplexers", IEEE Trans. Microwave Theory Tech., vol. MTT-37, pp. 340 - 350, Feb. 1989.
- [9] J. Bornemann, "A new class of E-plane integrated millimeter-wave filters", in IEEE MTT-S Int. Symp. Digest, pp. 599 - 602, 1989.
- [10] F. Arndt, I. Ahrens, U. Papziner, U. Wiechmann, and R. Wilkeit, "Optimized E-plane T-junction series power dividers", IEEE Trans. Microwave Theory Tech., vol. MTT-35, pp. 1052 - 1059, Nov. 1987.
- [11] S.J. Fiedziuszko, "Dual-mode dielectric resonator loaded cavity filters", IEEE Trans. Microwave Theory Tech., vol. MTT-30, pp. 1311-1316, Sept. 1982.
- [12] F. Arndt, T. Duschak, U. Papziner, and P. Rolappe, "Asymmetric iris coupled cavity filters with stopband poles", in IEEE MTT-S Int. Symp. Digest, pp. 215 - 218, 1990.